IEEE Access
Multidisciplinary | Rapid Review | Open Access Journal

Received March 20, 2019, accepted May 3, 2019, date of publication May 8, 2019, date of current version May 23, 2019.

Digital Object Identifier 10.1109/ACCESS.2019.2915533

Driving Fatigue Classification Based on Fusion Entropy Analysis Combining EOG and EEG

HONGTAO WANG[1,2], (Member, IEEE), CONG WU[1], TING LI[1], YUEBANG HE[1], PENG CHEN[1], AND ANASTASIOS BEZERIANOS[2]

[1]Faculty of Intelligent Manufacturing, Wuyi University, Jiangmen 529020, China
[2]Centre for Life Sciences, Singapore Institute for Neurotechnology, National University of Singapore, Singapore 117456

Corresponding authors: Hongtao Wang (nushongtaowang@qq.com) and Anastasios Bezerianos (tassos.bezerianos@nus.edu.sg)

This work was supported in part by the Defence Science Organisation (DSO), Singapore, under Grant R-719-000-027-592, in part by the Technology Development Project of Guangdong Province under Grant 2017A010101034, in part by the Science Foundation for Young Teachers of Wuyi University under Grant 2018td01, in part by the Natural Science Foundation of Guangdong Province under Grant 2018A030313882, in part by the Projects for International Scientific and Technological Cooperation under Grant 2018A05056084, and in part by the Jiangmen Brain-like Computation and Hybrid Intelligence R&D Center under Grant [2018]359 and Grant [2019]26.

ABSTRACT The rising number of traffic accidents has become a major issue in our daily life, which has attracted the concern of society and governments. To deal with this issue, in our previous study, we have designed a real-time driving fatigue detection system using power spectrum density and sample entropy. By using the wireless technology and dry electrodes for EEG collection, we further integrated virtual reality simulated driving environment, which made our study more applicable to realistic settings. However, the high accuracy of classification for driving fatigue has not been obtained. To measure the time series complexity of the EEG signal, we proposed a fusion entropy (sample entropy, approximate entropy, and spectral entropy) analysis method of EEG and EOG. First, a sample entropy was applied for feature extraction from the horizontal and vertical EOG. Second, an approximate entropy, sample entropy, and spectral entropy features of each sub-band of EEG are extracted. Third, feature fusion for sub-band is performed by canonical correlation analysis (CCA). Finally, the features of EOG and EEG are classified using a relevant vector machine (RVM). Twenty-two subjects participated in the driving fatigue experiments for a duration of 90 min. The results demonstrated that the fusion entropy analysis combining EOG and EEG could provide an alternative method for driving fatigue detection, and the average accuracy rate was up to $99.1 \pm 1.2\%$. The authors further analyzed the effect of feature fusion in four sub-bands (δ, α, β, and θ) and compared with every single sub-band on classification performance, it is proved that the former is superior to the latter presenting the proposed method can provide effective indicators for driving fatigue detection.

INDEX TERMS Driving fatigue, electroencephalogram (EEG), electrooculogram (EOG), sample entropy, approximate entropy, spectral entropy.

I. INTRODUCTION

The World Health Organization released a report that in 2015 more than 1.2 million young people died worldwide, with an average of more than 3,000 people per day. Traffic accidents are the number one killer of people between the ages of 10 and 19 [1]. With the rising number of traffic accidents in our daily life, the severity of this issue has attracted the concern of society and governments [2]. Other experts agree that driving fatigue is a significant cause of traffic accidents and is believed to account for 20-30% of all vehicle accidents [3]. Actually, it is a conservative estimate that the actual contribution of fatigue to road accidents may be much higher [4], [5]. As well known, driving fatigue is a feeling of extreme physical or mental tiredness which occurred after a long distance of continuous driving. It became a major factor to affect drivers resulting in slow reaction times, reduced vigilance and an irregular driving aptitude [6]. Therefore, the development of driving fatigue detection method that can identify the levels of mental fatigue accurately to prevent disastrous traffic events seems a crucial and urgent topic of study.

The associate editor coordinating the review of this manuscript and approving it for publication was Xun Chen.

Several research groups try to detect and quantify mental fatigue from the measurement of physiology variables such as electroencephalogram (EEG), electrooculogram (EOG), and electromyogram (EMG) [7]–[11]. Compared with machine vision based measures [12], [13], neurophysiology-based measures [14], [15] can provide an objective characterization of the state of the driver [16]. Among the numerous physiological indicators available to estimate the driver's fatigue level, the EEG signal has been proven to do a good job of mental state indicator [17]. Eoh et al. developed an algorithm based on the changes of in the major EEG bands including δ, α, β, θ to detect fatigue [18]. The performance of ratios of δ, θ, α and β activities interesting features to be detected with changes in the drowsiness level. Thus, four parameters θ/β, α/β, $(\alpha+\theta)/\beta$ and $(\alpha+\theta)/(\alpha+\beta)$ are used to fatigue prediction [19]. Nikita Gurudath et al. used a wavelet transform to extract sub-bands and calculated the mean, median, variance, standard deviation as features for drowsy driving detection [20]. Faramarz et al. only used the changes of α power for mental fatigue detection [21]. Entropy has also been applied to measure the changing complexity of electrophysiological signals [22], [23]. Zhang *et al.* realized an automated detection of driver fatigue system based on entropy and complexity measures [24]. Hassan and Bhuiyan carried out a series of research work about the identification of sleep states from EEG [25]–[32]. In our previous study, we proposed an integrated metric combined by averaging the powers spectrum density of $(\theta+\alpha)/\beta$ and θ/β to predict the driving fatigue. Furthermore, sample entropy was also applied to online driving fatigue detection [33].

EOG is another type of electrical signal generated by the eye movement and can be measured by the skin around the eyes. The magnitude of EOG varies according to the displacement of the eye ball from its resting location [34]. The EOG signals contain rich information, which can reflect the level of drowsiness directly [35], [36]. Bulling *et al.* found that the EOG signal caused by the movements of eyes is a good indicator of mental activities [37]. Zhang *et al.*, Zheng and Lu proposed different electrode placements on the forehead and extracted various eye movement features (EOG) for fatigue detection [38], [39].

Multi-modal system combing different kinds of signals has become a new trend of system design, the advantage is it can not only help to promote the robust of the system but also improve recognition accuracy [40]–[42]. In fact, several literatures have indicated that signals from different medals can reflect different aspects of mental states [39], [43]. As we are known, EEG is usually used to represent internal cognitive states, while EOG is commonly applied to reflect the external subconscious behaviors. The purpose of this paper is to fully excavate the complementary information provided by these two modalities and further to construct a more robust and accurate driving fatigue classification system by integrating EEG and EOG.

The remainder of this paper is organized as follows: Section II provides the paradigm of system and data acquisition. Section III provides methodology including signal preprocessing, feature extraction and classification. Experimental results are presented in Section V. Further discussions are presented in Section VI. The conclusion is presented in Section VII.

FIGURE 1. The simulated driving system used for the implementation of the proposed protocol.

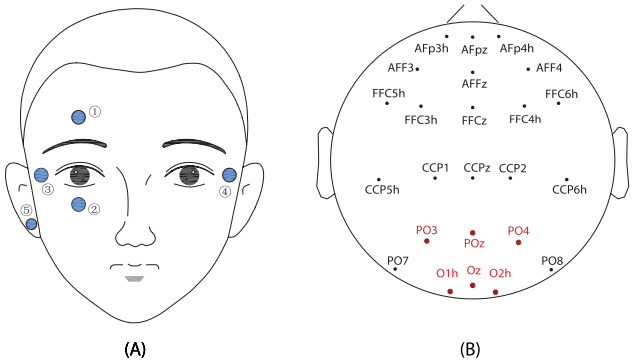

FIGURE 2. (A) The blue pair dots (1 and 2) and (3 and 4) indicate the electrodes placements for vertical and horizontal EOG collection respectively. (B) The names and positions of twenty-four dry EEG electrodes.

II. PARADIGM OF SYSTEM AND DATA ACQUISITION

As shown in Fig.1, the virtual reality simulated driving environment mainly consists of a simulated driving system and a wireless dry EEG acquisition system (Cognionics headset HD-72). In order to provide a more realistic sense of driving, the simulated driving system equipped with three 65 inches LCD screens, a Logitech G27 Racing Wheel simulator (a driving wheel, three pedals, and a six-speed gearbox) and a host computer which provides a driving environment. Twenty-four dry sensors integrated into the Cognionics headset are used to collect electroencephalogram from the subject's scalp and then the EEG signals are transferred wireless by a Bluetooth module transmitter. A host laptop (Toshiba Intel(R)Core(TM)i5-6200U Duo 2.4 *GHz*) is used to collect the EEG signals by a Bluetooth receiver for further processing and run a Cognionics software.

During signal collection, the EEG signals are referenced to both right and left mastoids, while EOG signals are referenced to the right ear. As shown in Fig.2 (A), the vertical and horizontal EOG are recorded by ECG Electrodes (Skintact products). In Fig.2(B), twenty-four standard dry electrodes are employed, which are placed at electrode sites

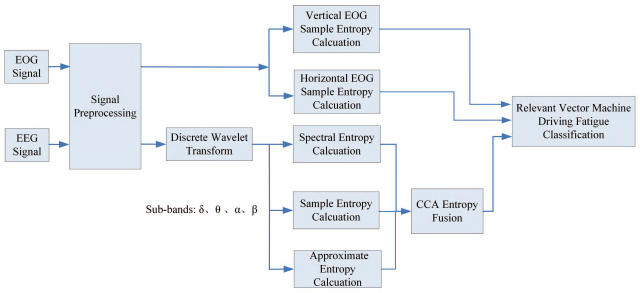

FIGURE 3. The flow chart of driving fatigue classification based on fusion entropy analysis method.

in the frontal, central, parietal, and occipital regions in accordance by a modified international 10-20 system of electrode placement [44]. In the present work, six channels (PO3, POz, PO4, O1h, Oz, O2h) marked red are used for EEG entropy calculation. All impedances are kept below 20 kΩ. EEG signals are amplified, sampled at a rate of 250 *Hz*, and band-pass filtered between 0.5 and 100 *Hz*, the parameters can be preset in the Cognionics software.

III. METHODOLOGY

As shown in Fig.3, the proposed driving fatigue classification based on fusion entropy analysis method mainly contains signal preprocessing, discrete wavelet transform for sub-bands extraction and noise suppression, fusion entropy feature extraction for EOG and EEG, and revelent vector machine based classification.

A. SIGNAL PREPROCESSING

The acquired data were processed and analyzed using EEGLAB [45] during the preprocessing stage. The preprocessing of EEG and EOG signals includes spatially filtered with common average reference (CAR) [46], de-trended, remove mean and then band-pass filtered at 0.01-32 *Hz*.

We applied the discrete wavelet transform (DWT) [47] to achieve EEG signal preprocessing with the following parameters: Daubechies wavelet of db4 [48] and decomposition level of six. DWT is particularly effective for representing various aspects of signals, such as trends, discontinuities, and repeated patterns, where other signal processing approaches fail or are not as effective [49]. The DWT decomposes a signal into a set of basic functions called Wavelets [22], [50]–[52]. The wavelet-packet decomposition at the j-th level of EEG signals given 2^j set of sub-band coefficients of length $\left\{P_{j,m}(n)\, k = 1, 2, ..., \frac{N}{2^j}\right\}$. These wavelet coefficient vectors reflet the change in the signal with time in the frequency:

$$\left[\frac{(m-1)\,F_s}{2^{j+1}}, \frac{mF_s}{2^{j+1}}\right] \tag{1}$$

where F_s is the sampling frequency, which is 250 *Hz* in this study and $m = 0, 1, ..., 2^{j-1}$. The frequency indexes range from 0 to $2^j - 1$ for zero to the Nyquist frequency (125 *Hz*) with an original sampling frequency of 250 *Hz*. The original signals were decomposed with a DWT of 6 levels, which is similar to our previous study [33]. In order to reconstruct the original signal, the inverse wavelet transform was applied to the wavelet coefficients. For example, δ band of the EEG signal was constructed using the wavelet coefficients $W_{6.0}$ - $W_{6.1}$. The reconstruction of θ, α and β band follows the same manner. As shown in Table 1, on the basis of frequency bands of extracted from the wavelet coefficients, the frequency bands δ, θ α and β are defined by acquiring the mean of corresponding frequency bands in relevant level. Thus the sub-bands EEG signals can be obtained for further analysis.

TABLE 1. Frequency bands extracted from the wavelet coefficients and grouped into corresponding frequency sub-bands (δ, θ, α, β).

Wavelet Coefficients	Frequency Range	Frequency Bands
$W_{6.0}$ -$W_{6.1}$	0.01-3.91 Hz	δ
$W_{6.2}$ -$W_{6.3}$	3.91-7.81 Hz	θ
$W_{6.4}$ - $W_{6.6}$	7.81-13.67 Hz	α
$W_{6.7}$ - $W_{6.15}$	13.67-31.25 Hz	β

B. FEATURE EXTRACTION

Five categories of features are extracted in the present study including (1) sample entropy calculated from vertical EOG, (2) sample entropy calculated from horizontal EOG, (3) spectral entropy calculated from EEG, (4) sample entropy calculated from EEG, (5) approximate entropy calculated from EEG. We use a sliding window with a length of 4 seconds and 1 second step to calculate the entropy of EEG from the selected six channels in the occipital region. Because in this region, a significant change in entropy and complexity could be found [24]. While a sliding window of 10 seconds and 1 second step to calculate the entropy of vertical and horizontal EOG respectively. The details of the feature extraction methods are as follows.

1) APPROXIMATE ENTROPY

approximate entropy (AppEn) is a nonlinear dynamic parameter, which can reflect the regularity of signals and is capable for complex system classification [24], [53]. Approximate entropy can be calculated by the following equations.

Let a time series containing N samples be $X = [x(1), x(2), ..., x(N)]$. Two sub-sequences of X can be given as follows:

$$\begin{aligned} X(i) &= [x(i), x(i+1), ..., x(i+m-1)], \\ &\quad 1 \le i \le N-m+1 \\ X(j) &= [x(j), x(j+1), ..., x(j+m-1)], \\ &\quad 1 \le i \le N-m+1 \end{aligned} \tag{2}$$

Define the distance between any two m-dimensional vectors $X(i)$ and $X(j)$ as:

$$d|X(i), X(j)| = \max|x(i+k) - x(j+k)| \tag{3}$$

Define a threshold $r = k \times SD, (r > 0)$, which represent the noise filter level. $r = 0.2$ in the present work and SD is the standard deviation of the time series. $num\{d|X(i), X(j)| \leq r\}$ is the number of statistics for each $1 \leq i \leq N - m + 1$, which meet the condition of $d|X(i), X(j)| \leq r$, and the ratio of its total length to the vector $C_i^m(r)$ is recorded as follows:

$$C_i^m(r) = \frac{1}{N-m+1} * num\{d|X(i), X(j)| \leq r\} \quad i = 1, ..., N-m+1, \quad i \neq j \tag{4}$$

$C_i^{m+1}(r)$ can be obtained in the similar way above.

$$C_i^{m+1}(r) = \frac{1}{N-m+1} * num\{d|X(i), X(j)| \leq r\} \quad i = 1, ..., N-m+1, \quad i \neq j \tag{5}$$

$AppEn(m, r, N)$ is defined as follows:

$$AppEn(m, r, N) = \frac{1}{N-m+1} \sum_{i=1}^{N-m+1} \log C_i^m(r) - \frac{1}{N-m} \sum_{i=1}^{N-m} \log C_i^{m+1}(r) \tag{6}$$

2) SAMPLE ENTROPY

Sample entropy (SamEn) is an improved method of AppEn [54], which is given by the following equation.

$$SamEn(m, r, N) = -\ln \frac{B^{m+1}(r)}{B^m(r)} \tag{7}$$

Define $B^m(r)$ as

$$B^m(r) = \frac{1}{N-m} \sum_{i=1}^{N-m} C_i^m(r) \tag{8}$$

In this study, the parameters are typically chosen as $m = 2$ and $r = 0.2 * SD$.

3) SPECTRAL ENTROPY

Spectral entropy (SpeEn) has shown the potential on EEG signal processing [55]. There are three steps for SpeEn calculation. Firstly, estimate the parameters of the model-based method from a given data sequence $x(n)$, $0 \leq n \leq N - 1, N = 2500$. Secondly, compute the PSD estimated from these estimations. Thirdly, Shannon transformation.

Step one: The AR method is based on modeling the data sequence $x(n)$ as the output of a causal and discrete filter whose input is white noise, which is expressed as below.

$$x(n) = -\sum_{k=1}^{p} a(k)\, x(\text{n-k}) + \omega(n) \tag{9}$$

where $a(k)$ is the AR coefficient, $x(n)$ is the white noise of variance equal to σ^2, and p is the order of the AR model. In this work, AR coefficients are estimated by the recursive Burg method, which is based on minimizing the forward and backward prediction errors. From the estimation of AR parameters by the Burg algorithm, PSD estimation is formed as [56].

$$\hat{P}_{burg}(f) = \frac{\hat{e}_p}{\left|1 + \sum_{k=1}^{p} \hat{a}_p(k)\, e^{-j\pi fk}\right|} \tag{10}$$

where $\hat{e}_p$ is the total least squares error. The model order p of AR method is determined by using the Akaike information criterion (AIC) [57]. In this study, the model order is taken as $p = 10$.

Step two: Then the PSD results of each frequency band are normalized to obtain the relative PSD of one band to the whole frequency band.

$$P_{relative} = \frac{\sum_{f=f_1}^{f=f_2} P(f)}{\sum_{f=f_L}^{f=f_H} P(f)} \tag{11}$$

where $[f_L, f_H] = [0.1, 31.25]$ and $[f_1, f_2]$ is determined by the frequency sub-band selected according to $\delta, \alpha, \beta, \theta$.

Step three: Following normalization, the corresponding spectral entropy is defined according to Shannon transformation:

$$H(f) = Q(f) * \log \frac{1}{Q(f)} \tag{12}$$

The formula for calculating the SpeEn is as follows:

$$SpeEn = \frac{\sum_f H(f)}{\log(N(f))} \tag{13}$$

4) FEATURE FUSION BASED ON CCA

Consider two n-dimensional variables X and Y, their linear combinations can be presented by $x = x^T W_x$ and $y = y^T W_y$ respectively. We use CCA to find the weight vectors W_x and W_y that maximize the correlation between x and y to keep their independent as much as possible.

$$\max_{Wx, Wy} \rho(x, y) = \frac{E\left[x^T y\right]}{\sqrt{E\left[x^T x\right] E\left[y^T y\right]}} = \frac{E\left[W_x^T X Y^T W_y\right]}{\sqrt{E\left[W_x^T X X^T W_x\right] E\left[W_y^T Y Y^T W_y\right]}} \tag{14}$$

where the maximum of ρ with respect to W_x and W_y is the maximum canonical correlation, T means transposed matrix.

Finally, the feature fusion is as follows

$$F = W_x * W_x^T * x + W_y * W_y^T * y \tag{15}$$

In the present work, there are five types of entropies totally. For EEG entropy calculation, we can get three types of EEG entropies from the sliding window of 4 s, they are spectral entropy, sample entropy and approximate entropy respectively. Furthermore, the EEG signals in δ, α, β and θ bands are applied in entropy calculation and result in twelve EEG entropy features. They are $\delta_{SpeEn}, \delta_{SamEn}, \delta_{AppEn}, \alpha_{SpeEn}, \alpha_{SamEn}, \alpha_{AppEn}, \beta_{SpeEn}, \beta_{SamEn}, \beta_{AppEn}, \theta_{SpeEn}, \theta_{SamEn}, \theta_{AppEn}$ respectively. Using equation (14)- (15), we can obtain the

fusion entropy with four dimensions for each EEG segments. While for EOG entropy calculation, we can get two types of EOG entropies from the sliding window of 10 *s*, they are sample entropy calculated from vertical EOG ($Vertical_{SamEn}$) and sample entropy calculated from horizontal EOG ($Horizonal_{SamEn}$). Finally, the six dimension entropy combing EEG and EOG to component a new vector, which can be fed to the RVM classifier.

C. CLASSIFICATION

Relevant vector machine was applied for the alert state and fatigue state classification. Details for the two classes classification are shown as follows: Given an input variable x, to get its posterior probability relative to each class. According to the theory of generalized linear models, the logical *sigmoid* link function $\sigma(y) = 1/1+\exp(-y)$ is introduced for $y(x; w)$ making $P(t|x)$ obey the Bernoulli distribution. Thus the probability prediction of the input variable objective function is:

$$p(t_i = 1|w) = \sigma(y(x_i; w)) = \frac{1}{1 + \exp(-y(x_i; w))} \quad (16)$$

where $y(x_i; \omega) = \sum_{n=1}^{N} \omega_n K(x, x_i) + \omega_0$, ω_n are the weights, $K(x, x_i)$ is the kernel function.

Assuming that the variables are distributed independently, the likelihood function can be obtained as follows:

$$p(t|w) = \prod_{i=1}^{N} \sigma\{y(x_i; w)\}^{t_i} * [1 - \sigma\{y(x; w)\}]^{1-t_i} \quad (17)$$

where w is the weight and the target value is $t_i \in \{0, 1\}$. Michael E. Tipping Proposed a Laplace approximation procedure to solves the above equation, and the steps are as follows [58]:

Step one: Given the iteration position of the model posterior distribution, for the current parameter with the fixed value α,the weight with the highest probability of w_{MP} can be obtained. Follow the of Bayesian theory $p(w|t, \alpha) \propto p(t|w)p(w|\alpha)$, we can get:

$$\begin{aligned} w_{MP} &= \arg\max_w (w|t, \alpha) = \arg\max_w \frac{p(t|w)p(w|\alpha)p(\alpha)}{p(\alpha|t)} \\ &= \arg\max_w p(t|w)p(w|\alpha) = \arg\max_w \log p(t|w)p(w|\alpha) \end{aligned} \quad (18)$$

That is, w_{MP} is obtained when maximizing the formula.

$$\begin{aligned} &\log p(t|w)p(w|\alpha) \\ &= \sum_{i=1}^{N} [t_i \log y_i + (1 - t_i) \log(1 - y_i)] - \frac{1}{2} w^T A w \end{aligned} \quad (19)$$

where $A = diag(\alpha_0, \alpha_1, ..., \alpha_N)$, $y_i = \sigma\{y(x_i; w)\}$. The above formula is a logical likelihood function with a penalty term, and it can be able to obtain extreme values under repeated iterations. The Hessian matrix of the formula (19) can be calculated in the next step, using the Newton method, which is an effective method [59].

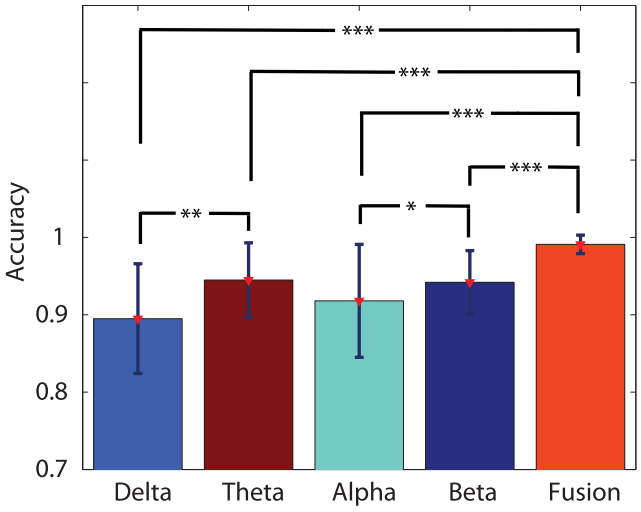

FIGURE 4. Performance comparison of classification on features of the sub-bands entropy (EEG+EOG) and fusion entropy (EEG+EOG).

Step two: The Laplace method is a quadratic approximation of the logical posterior. Perform first-order and two-order differentials by formula (19) and then we can get:

$$g = \nabla_w \log[p(t|w)p(w|\alpha)] = \Phi^T(t - y) - Aw \quad (20)$$

where Φ is a basic function.

$$\begin{aligned} \Phi &= [\phi(x_1), \phi(x_2), ..., \phi(x_N)] \\ \Phi(x_n) &= [1, K(x_n, x_1), K(x_n, x_2), ..., K(x_n, x_N)]^T \\ H &= \nabla_w \nabla_w \log[p(t|w)p(w|\alpha)] = (-\Phi^T B \Phi - A)^{-1} \end{aligned} \quad (21)$$

$$\Delta w = -H^{-1} g \quad (22)$$

$$w_{MP}^{new} = w_{MP} + \Delta w \quad (23)$$

where $y = [y_1, y_2, ..., y_N]^T$, $B = diag(\beta_1, \beta_2, ..., \beta_N)$, $\beta_n = \sigma[y(x_n)]\{1 - \sigma[y(x_n)]\}$, H is a Hessian matrix and covariance matrix $\sum$ can be obtained.

$$\sum = -H = (\Phi^T B \Phi + A)^{-1} \quad (24)$$

Step three: Using the first-order reciprocal $g = 0$ and the formula (24) of the logical posterior distribution, we can get:

$$w_{MP} = \sum \Phi^T B t \quad (25)$$

Using Gaussian approximation statistic $\sum$ and w_{MP} (instead of μ) and continuously update the parameters, the expression of the terminator is obtained as follows:

$$y_*(X_*, W_{MP}) = \Phi(X_*) W_{MP} \quad (26)$$

Substituting the result into the formula (16), we can get the probability that the test points belong to the classes 1 and 0 respectively. Then according to the probability value $p(t_* = 1|x_*)$ and $p(t_* = 0|x_*)$ determines the classification category of x_*.

In addition, the choice of kernel function determines the way the sample is mapped from low-dimensional space to

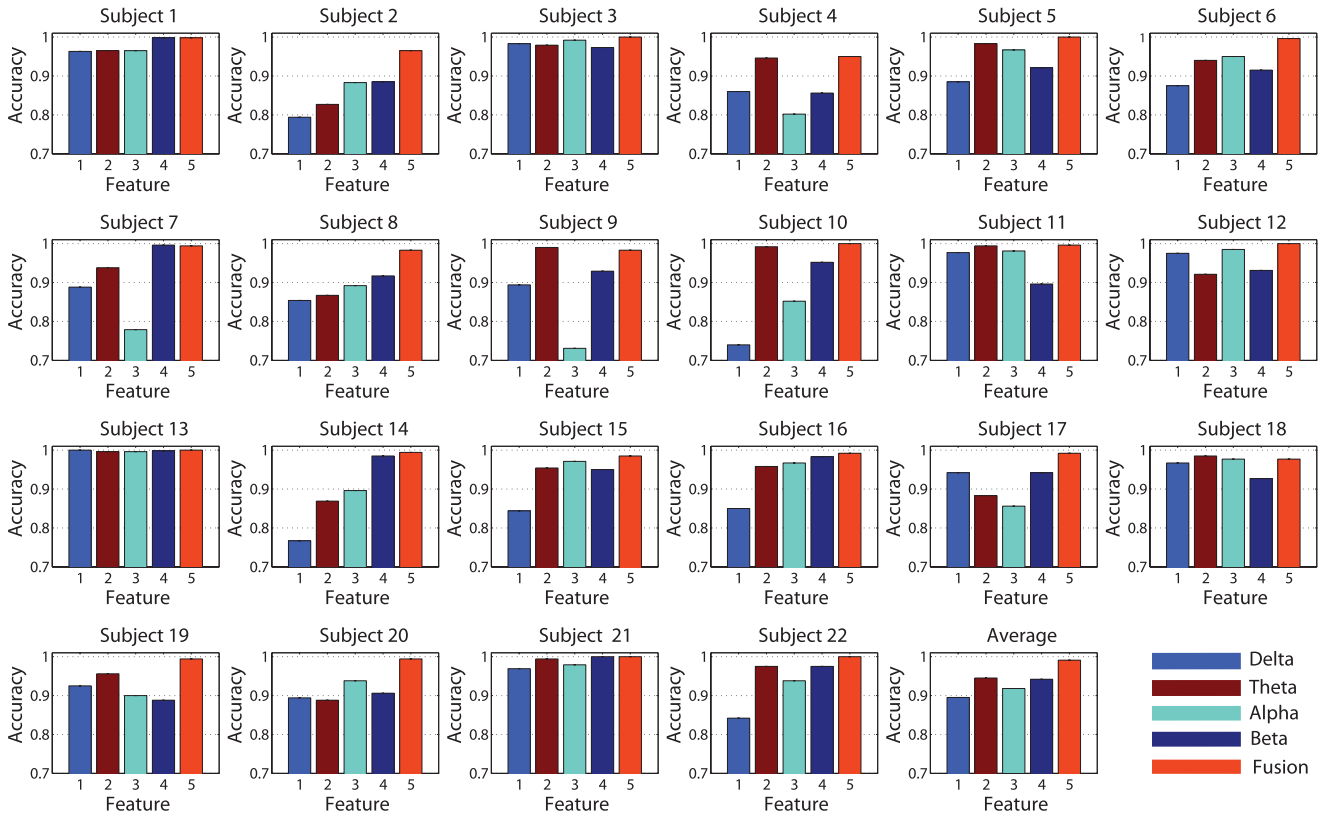

FIGURE 5. The classification performance of the RVM based on sub-bands using different features (sample entropy, approximate entropy and spectral entropy) for subject 1 to subject 22.

high-dimensional space. The comprehensive performance of learning has a great impact. The kernel function chosen in this paper is a radial basis function (RBF).

$$K(x, x_i) = exp\left(-g \|x - x_i\|^2\right) \tag{27}$$

IV. EXPERIMENTAL PROTOCOL

A. PARTICIPANTS

To evaluate the performance of the proposed method, twenty-two healthy subjects (seventeen males and five females) from National University of Singapore participated in the driving fatigue experiments at the Cognitive Engineering Laboratory of Singapore Institute for Neurotechnology (SINAPSE). All the experiments were carried out in the afternoon from 3 pm to 5 pm, as it was easier to induce fatigue. These participants are 21.5 ± 1.5 years old with right-handed and have a normal or corrected-to-normal vision. Before the experiment, participants were asked to refrain from consuming caffeine and alcohol approximately four h and alcohol 24 h and reported compliance with these instructions.

B. DRIVING EXPERIMENTAL TASK

The driving experimental task is designed similar to the protocol being followed in our previous work [33], [60], [61]. The subject set in the front of the screen for a distance of 1.8 *meters*, these screens display the landscape along the road

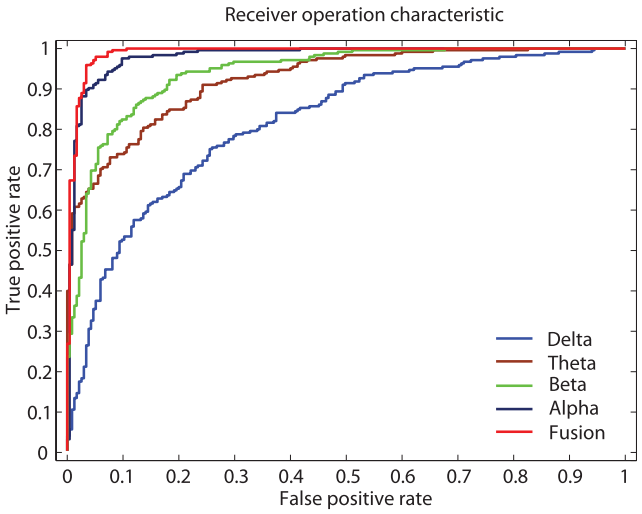

FIGURE 6. Receiver operation characteristic of RVM for the subject 6 under different sub-bands features.

and obey to the left driving rules according to Singapore standards. The driving experiment is a continuous task which lasts for lasted 1.5 h. The participants were instructed to drive a stimulated car at a pre-set constant speed of 80 km/h, and follow a guided car in a two-way rural road without crossroads. A questionnaire is completed by the participant independently according to the NASA task load index [62]

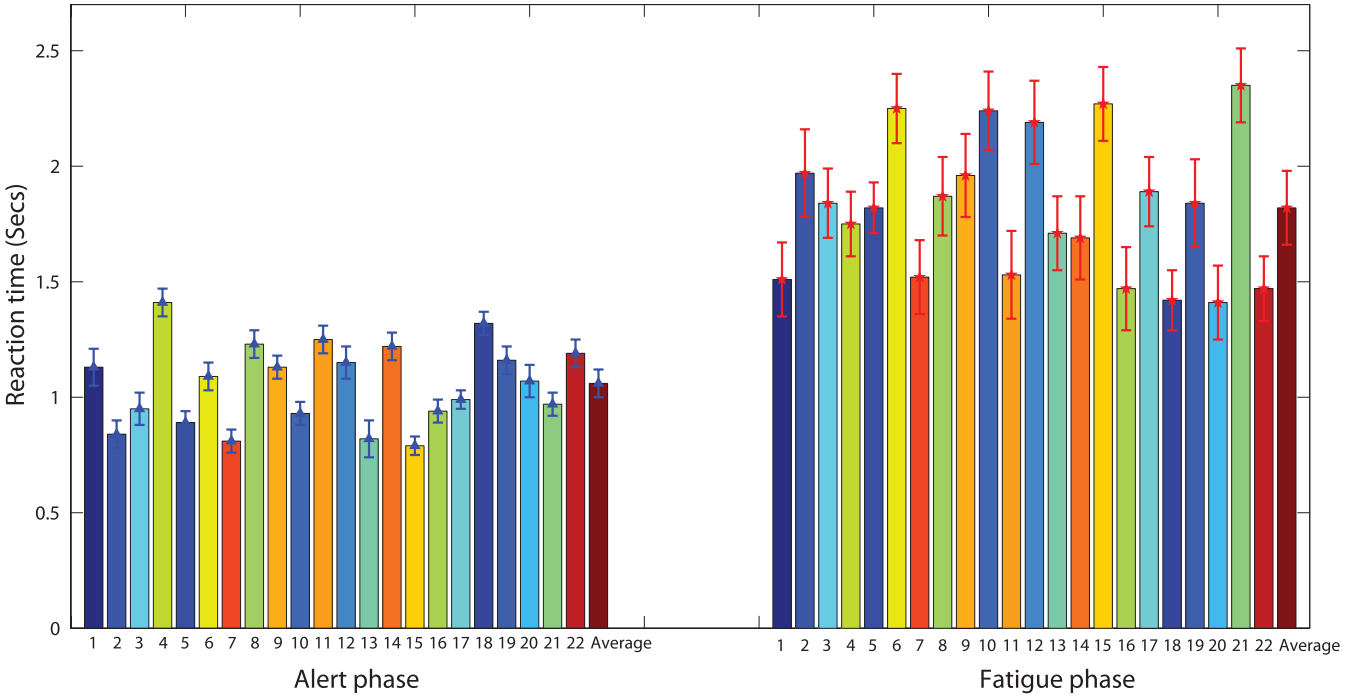

FIGURE 7. The classification performance of the RVM based on different features for subject 1 to subject 22.

C. OFF LINE DATA ANALYSIS

The duration of each experiment was 90 minutes and no one quit the experiment because he/she was not exhausted enough to sleep. From the NASA task load index provided by the participants, the values of "Mental demand" and "Frustration" are 79 ± 5 and 65 ± 7, which indicates that most participants perceived mental fatigue at the end of driving experiments. Thus, in off line analysis, the first and last 10 minutes (more than 10 minutes actually) were extracted for further analysis, which are labeled to alert phase and fatigue phase respectively. More detail, for the first 10 minutes, we used a sliding window of 4 seconds overlapping 3 seconds resulting in 600 segments for EEG analysis. Meanwhile, we used a sliding window of 10 seconds overlapping 9 seconds resulting in 600 segments for EOG analysis. For the last 10 minutes, we applied the same process sequence according to the first 10 minutes. Finally, 1200 samples for each subject were obtained and then be stored in random order. For the driving fatigue classification, a cross-validation approach [63] was applied for the RVM training and classification (60% for training, 40% for testing).

V. RESULTS

We compared the performance of RVM classifier on different EEG entropy features extracted from different frequency sub-bands ($\delta, \alpha, \beta, \theta$) and EOG entropy features. The averaged accuracy and standard deviations for twenty-two subjects are shown in Fig.4, which are $89.5 \pm 7.1\%$, $94.5 \pm 4.8\%$, $91.8 \pm 7.3\%$, $94.2 \pm 4.1\%$ and $99.1 \pm 1.2\%$ under four sub-bands entropy (EEG+EOG) and fusion entropy (EEG+EOG) respectively. The statistical significance of the entropy features was estimated by the two-tailed student-test across all the five features [64]. The p-value from the Student-test shows that the significantly different exist between the fusion entropy and the sub-bands entropy($p < 0.001$). A significance level of $p < 0.01$ was observed between δ band entropy features and θ band entropy features, while $p < 0.05$ is for α band entropy features and β band entropy features. Furthermore, at the aim of providing more details about the classification results, the accuracies obtained on different entropy features for each subject are shown in Fig.5. The bars and the error bars represent the average accuracies and standard deviations respectively. Asterisks indicate the significance levels of accuracy differences between different features. (* $p < 0.05$, ** $p < 0.01$, *** $p < 0.001$).

The receiver operation characteristic (ROC) curve depicts the relationship between the two rates of true positive rate (TPR) and false positive rate (FPR) [65]. True positive (TP) presents the number of a fatigue sample is recognized as a fatigue state. True negative (TN) presents the number of an alert sample is recognized as an alert state. False positive (FP) presents the number of a fatigue sample is recognized as an alert state. False negative (FN) presents the number of an alert sample is recognized as a fatigue state. TPR and FPR can be defined as follows,

$$TPR = \frac{TP}{TP + FN}$$
$$FPR = \frac{FP}{FP + TN} \tag{28}$$

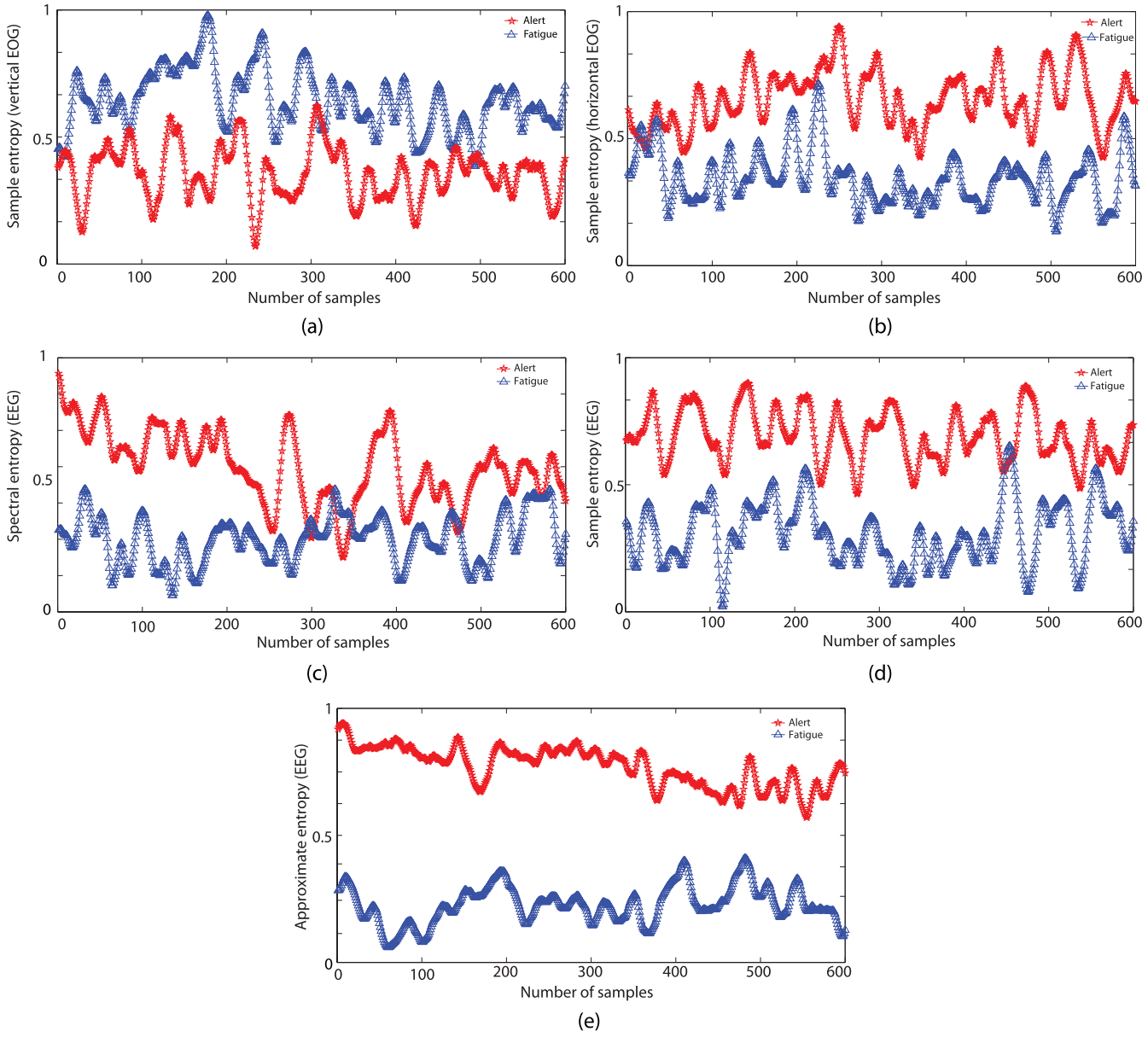

FIGURE 8. The values of different entropies averaged by all twenty-two participants.

In order to show the performance of RVM classifier on different entropy features extracted from different frequency sub-bands (δ, α, β, θ) clearly, we calculated the ROC curve for the subject 6 as an example shown in Fig.6.

VI. DISCUSSION

A. REACTION TIME

During the online experiment, reaction time has been recorded as a behavior index, which can reflect the level of fatigue. It is defined as the visual stimuli of a break signal make by the guided car and the break signal made by the participant. Thus we extracted the reaction time which obtained in the first 10 mins and last 10 mins for twenty-two subjects respectively. As shown in Fig.7, for each subject the averaged reaction time in the last 10 mins obviously increase compared with the averaged reaction time in the first 10 mins. It revealed that after 90 mins driving experiment, for all the subject have changed form alert phase to fatigue phase. The averaged reaction time for twenty-two subjects during the first 10 mins and the last 10 mins are $1.06 \pm 0.06\%$ secs and $1.82 \pm 4.8\%$ secs, respectively.

B. ENTROPY ANALYSIS

In the present study, five categories of entropies were applied for driving fatigue classification as shown in Fig.8. Fig.8(a) and (b) show the sample entropy calculated from vertical EOG and horizontal EOG. The red asterisks stand for the sample entropy calculated from the alert phase, while the blue triangles represent the sample entropy calculated from the fatigue phase. There are 600 samples for each phase.

TABLE 2. The classification performance of the RVM based on sub-bands using different features (sample entropy, approximate entropy and fuzzy entropy) for subject 1 to subject 22.

Subject	Delta (%)	Theta (%)	Alpha (%)	Beta (%)	Fusion (%)
S1	89.7	92.8	89.7	95.3	98.9
S2	65.8	67.5	62.8	83.9	87.5
S3	96.1	95.3	100	98.1	100
S4	88.9	94.2	72.5	74.7	91.9
S5	84.2	94.2	91.9	87.2	99.2
S6	85	86.1	90.8	80	98.3
S7	82.8	93.6	75	99.4	98.6
S8	85	79.2	82.5	84.2	95.3
S9	88.9	100	70.6	80	98.3
S10	74.7	98.6	89.2	94.2	100
S11	81.1	95.6	87.8	88.6	99.2
S12	96.7	92.8	99.4	93.3	100
S13	100	100	98.6	98.9	100
S14	78.6	77.5	83.6	93.3	97.5
S15	83.9	82.2	81.7	80	96.4
S16	81.7	90	83.6	71.4	96.7
S17	89.7	90.3	83.9	89.7	98.9
S18	94.2	95.6	95.6	76.9	98.6
S19	81.7	81.1	85.6	83.6	99.7
S20	88.3	83.1	98.6	92.8	98.1
S21	95.3	99.4	98.9	97.2	100
S22	85	96.9	93.6	97.2	100
$Mean \pm std$	86.2±7.8	90.3±8.6	87.1±10.2	88.2±8.5	97.9±3

Additionally, the sample entropy for vertical EOG calculated from the alert phase is bigger than the fatigue phase, which indicates that the frequency of eye-blink became higher when the participant feels mental fatigue. However, the NASA task load questionnaire and the statistics reaction time showed the subject was not exhaust enough to sleep, which means these participants have not entered the excessive fatigue phase. Thus the decrease pattern of eye-blink has not been observed. The sample entropy for horizontal EOG calculated from the alert phase is smaller than the fatigue phase, which indicates that the movement of eyes became slow and the participant unwilling or delay to pay attention the outside environment when he/she feels mental fatigue. Another study also proved that when a person enters into the fatigue state eye movement decreases while the blink rate increases [66].

Fig.8(a)-(e) represent sample entropy calculated from vertical EOG of the alert and fatigue phase, sample entropy calculated from horizontal EOG of the alert and fatigue phase, spectral entropy calculated from EEG of the alert and fatigue phase, sample entropy calculated from EEG of the alert and fatigue phase and approximate entropy calculated from EEG of the alert and fatigue phase respectively. In Fig.8(c),(d) and (e), with the time on task of driving, for most participants the entropies (spectral entropy, sample entropy and approximate entropy) in occipital area present an obvious decrease pattern resulting in the values of the alert stare are much higher than the fatigue state, especially for the approximate entropy. This result well agrees with our previous study [33] and Chi Zhang's study [24]. More importantly, this phenomenon reveals that with the depth of mental fatigue the complexity of EEG signal in the occipital area reduced.

Furthermore, we have tried using fuzzy entropy [67] as an alternative method of spectral entropy under the same test environment. Experiment results prove that fusion of different features can enhance the performance of the detection system [22], [68]. As shown in Table 3 and Fig.5, the performance sub-bands fusion entropy (sample entropy, approximate entropy and fuzzy entropy) analysis of EEG and EOG is not superior than the sub-bands fusion entropy (sample entropy, approximate entropy and spectral entropy) analysis (97.9 $\pm$ 3% vs. 99.1 $\pm$ 1.2%). Even fuzzy entropy is robust [69], it is shown that spectral entropy is more sensitive to fatigue-related EEG analysis.

C. COMPARISON OF DIFFERENT DRIVER FATIGUE DETECTION METHODS

In this paper, we proposed a fusion entropy (sample entropy, approximate entropy and spectral entropy) analysis of EEG and EOG for driving fatigue classification was proposed in this paper. Obviously, the simultaneous usage of EEG and

TABLE 3. Summary of relevant research works in the field of driver fatigue detection using different methods.

Research work	Channels	Approach (features)	Classifier	Average accuracy(%)	Type
Correa et al. [70]	C3-O1, C4-A1 and O2-A1	Multi-modal Analysis	Neural netwoks	83.6	Wet
Ko et al. [71]	A single frontal channel	Fast Fourier Transformation	The linear regression	90.0	Wet
Xiong et al. [72]	P3	Approximate entropy and sample entropy	Support vector machine	90.0	Wet
Chai et al. [73]	All channels	Autoregressive model	Sparse-DBN	93.1	Wet
Nguyen et al. [74]	All channels	Statistical tests	Fisher's linear discriminant	88.6	Wet
Hu et al. [75]	TP7	Fuzzy entropy	Gradient boosting decision tree	94.0	Wet
Our work	EEG (PO3, POz, PO4, O1h, Oz, O2h) and EOG	Sample entropy, approximate entropy and fuzzy entropy	Relevant vector machine	97.9±3	Dry
Our work	EEG (PO3, POz, PO4, O1h, Oz, O2h) and EOG	Sample entropy, approximate entropy and spectral entropy	Relevant vector machine	99.1±1.2	Dry

EOG signals can increase the accuracy of identification and classification results. A summery of the recent typical studies about driving fatigue classification are shown in Table 3. Compered with the existing systems and methodology, our system is vast superior in higher classification rate and wireless dry EEG and EOG collection, which make it a further step in a realistic application.

VII. CONCLUSION

In this paper, to measure the time series complexity of EEG signal, fusion entropy (sample entropy, approximate entropy and spectral entropy) analysis of EEG and EOG for driving fatigue classification was proposed. Twenty-two subjects participated in the fatigue driving experiments for a duration of 90 minutes. The experimental results demonstrated that the fusion entropy analysis combining EOG and EEG could provide an effective method for driving fatigue detection, and the average accuracy rate was up to $99.1 \pm 1.2\%$. For the sub-bands entropy, the averaged accuracy and standard deviations are $89.5 \pm 7.1\%$, $94.5 \pm 4.8\%$, $91.8 \pm 7.3\%$ and $94.2 \pm 4.1\%$ respectively. More interestingly, firstly we found that when a person enters into the mental fatigue state his/her eye movement decreases while eye blink rate increases. Secondly, higher classification accuracy rate has been obtained by sub-bands entropy fusion by simultaneous usage of hybrid EEG and EOG signals. Thirdly, the p-value from the Student-test shows that the significantly different exist between the fusion entropy features and the sub-bands (δ, α, β, θ) entropy ($p < 0.001$).

REFERENCES

[1] World Health Organization. (2017). Prieiga Per Internetą. *More Than 1.2 Million Adolescents Die Every Year, Nearly All Preventable*. [Online]. Available: http://www.who.int/mediacentre/news/releases/2017/yearly-adolescentdeaths/en

[2] A. Williamson, D. A. Lombardi, S. Folkard, J. Stutts, T. K. Courtney, and J. L. Connor, "The link between fatigue and safety," *Accident Anal. Prevention*, vol. 43, no. 2, pp. 498–515, 2011.

[3] P. S. Rau, "Drowsy driver detection and warning system for commercial vehicle drivers: Field operational test design, data analyses, and progress," Nat. Highway Traffic Saf. Admin., Washington, DC, USA, Tech. Rep. 05-0192, 2005.

[4] C. Zhao, C. Zheng, M. Zhao, J. Liu, and Y. Tu, "Automatic classification of driving mental fatigue with EEG by wavelet packet energy and KPCA-SVM," *Int. J. Innov. Comput.*, vol. 7, no. 3, pp. 1157–1168, 2011.

[5] H. Koch *et al.*, "Automatic sleep classification using a data-driven topic model reveals latent sleep states," *J. Neurosci. Methods*, vol. 235, pp. 130–137, Sep. 2014.

[6] R. N. Khushaba, S. Kodagoda, S. Lal, and G. Dissanayake, "Driver drowsiness classification using fuzzy wavelet-packet-based feature-extraction algorithm," *IEEE Trans. Biomed. Eng.*, vol. 58, no. 1, pp. 121–131, Jan. 2011.

[7] K. Hirvonen, S. Puttonen, K. Gould, J. Korpela, V. F. Koefoed, and K. Müller, "Improving the saccade peak velocity measurement for detecting fatigue," *J. Neurosci. Methods*, vol. 187, no. 2, pp. 199–206, 2010.

[8] B. Mandal, L. Li, G. S. Wang, and J. Lin, "Towards detection of bus driver fatigue based on robust visual analysis of eye state," *IEEE Trans. Intell. Transp. Syst.*, vol. 18, no. 3, pp. 545–557, Mar. 2017.

[9] H. Wang, C. Zhang, T. Shi, F. Wang, and S. Ma, "Real-time eeg-based detection of fatigue driving danger for accident prediction," *Int. J. Neural Syst.*, vol. 25, no. 2, pp. 643–651, 2015.

[10] L. H. Chew, J. Teo, and J. Mountstephens, "Aesthetic preference recognition of 3D shapes using eeg," *Cognit. Neurodyn.*, vol. 10, no. 2, pp. 165–173, 2016.

[11] C. Zhao, M. Zhao, Y. Yang, J. Gao, N. Rao, and P. Lin, "The reorganization of human brain networks modulated by driving mental fatigue," *IEEE J. Biomed. Health Informat.*, vol. 21, no. 3, pp. 743–755, May 2017.

[12] J. Jo, S. J. Lee, H. G. Jung, K. R. Park, and J. Kim, "Vision-based method for detecting driver drowsiness and distraction in driver monitoring system," *Opt. Eng.*, vol. 50, no. 12, pp. 13202–13209, 2011.

[13] J. Jo, S. J. Lee, K. R. Park, I.-J. Kim, and J. Kim, "Detecting driver drowsiness using feature-level fusion and user-specific classification," *Expert Syst. Appl.*, vol. 41, no. 4, pp. 1139–1152, Mar. 2014.

[14] R. Panicker, S. Puthusserypady, and Y. Sun, "An asynchronous P300 BCI with SSVEP-based control state detection," *IEEE Trans. Biomed. Eng.*, vol. 58, no. 6, pp. 1781–1788, Jun. 2011.

[15] P. Atchley, M. Chan, and S. Gregersen, "A strategically timed verbal task improves performance and neurophysiological alertness during fatiguing drives," *Hum. factors*, vol. 56, no. 3, pp. 453–462, 2014.

[16] K. LaFleur, K. Cassady, A. Doud, K. Shades, E. Rogin, and B. He, "Quadcopter control in three-dimensional space using a noninvasive motor imagery-based brain–computer interface," *J. Neural Eng.*, vol. 10, no. 4, pp. 1308–1326, 2013.

[17] C.-H. Chuang, C.-S. Huang, L.-W. Ko, and C.-T. Lin, "An EEG-based perceptual function integration network for application to drowsy driving," *Knowl.-Based Syst.*, vol. 80, pp. 143–152, May 2015.

[18] H. J. Eoh, M. K. Chung, and S.-H. Kim, "Electroencephalographic study of drowsiness in simulated driving with sleep deprivation," *Int. J. Ind. Ergonom.*, vol. 35, no. 4, pp. 307–320, 2005.

[19] B. T. Jap, S. Lal, P. Fischer, and E. Bekiaris, "Using EEG spectral components to assess algorithms for detecting fatigue," *Expert Syst. Appl.*, vol. 36, no. 2, pp. 2352–2359, 2009.

[20] N. Gurudath and H. B. Riley, "Drowsy driving detection by EEG analysis using wavelet transform and K-means clustering," *Procedia Comput. Sci.*, vol. 34, pp. 400–409, 2014.

[21] F. Gharagozlou *et al.*, "Detecting driver mental fatigue based on EEG alpha power changes during simulated driving," *Iranian J. Public Health*, vol. 44, no. 12, pp. 1693–1702, 2015.

[22] M. Kumar, R. B. Pachori, and U. R. Acharya, "Automated diagnosis of atrial fibrillation ECG signals using entropy features extracted from flexible analytic wavelet transform," *Biocybern. Biomed. Eng.*, vol. 38, no. 3, pp. 564–573, 2018.

[23] S. Nalband, A. Prince, and A. Agrawal, "Entropy-based feature extraction and classification of vibroarthographic signal using complete ensemble empirical mode decomposition with adaptive noise," *IET Sci., Meas. Technol.*, vol. 12, no. 3, pp. 350–359, 2017.

[24] C. Zhang, H. Wang, and R. Fu, "Automated detection of driver fatigue based on entropy and complexity measures," *IEEE Trans. Intell. Transp. Syst.*, vol. 15, no. 1, pp. 168–177, Feb. 2014.

[25] A. R. Hassan and M. I. H. Bhuiyan, "Computer-aided sleep staging using complete ensemble empirical mode decomposition with adaptive noise and bootstrap aggregating," *Biomed. Signal Process. Control*, vol. 24, pp. 1–10, Feb. 2016.

[26] A. R. Hassan and M. I. H. Bhuiya, "Automatic sleep scoring using statistical features in the EMD domain and ensemble methods," *Biocybernetics Biomed. Eng.*, vol. 36, no. 1, pp. 248–255, 2016.

[27] A. R. Hassan and A. Subasi, "A decision support system for automated identification of sleep stages from single-channel EEG signals," *Knowl.-Based Syst.*, vol. 128, pp. 115–124, Jul. 2017.

[28] A. R. Hassan and M. I. H. Bhuiyan, "An automated method for sleep staging from EEG signals using normal inverse Gaussian parameters and adaptive boosting," *Neurocomputing*, vol. 219, pp. 76–87, Jan. 2017.

[29] A. R. Hassan, "Computer-aided obstructive sleep apnea detection using normal inverse Gaussian parameters and adaptive boosting," *Biomed. Signal Process. Control*, vol. 29, pp. 22–30, Aug. 2016.

[30] A. R. Hassan and M. A. Haque, "Computer-aided obstructive sleep apnea screening from single-lead electrocardiogram using statistical and spectral features and bootstrap aggregating," *Biocybern. Biomed. Eng.*, vol. 36, no. 1, pp. 256–266, 2016.

[31] A. R. Hassan and M. A. Haqu, "Computer-aided obstructive sleep apnea identification using statistical features in the EMD domain and extreme learning machine," *Biomed. Phys. Eng. Express*, vol. 2, no. 3, p. 035003, 2016.

[32] A. R. Hassan and M. A. Haque, "An expert system for automated identification of obstructive sleep apnea from single-lead ECG using random under sampling boosting," *Neurocomputing*, vol. 235, pp. 122–130, Apr. 2017.

[33] H. Wang, A. Dragomir, N. I. Abbasi, J. Li, N. V. Thakor, and A. Bezerianos, "A novel real-time driving fatigue detection system based on wireless dry EEG," *Cogn. Neurodyn.*, vol. 12, no. 4, pp. 365–376, Feb. 2018.

[34] P. Malmivuo, J. Malmivuo, and R. Plonsey, *Bioelectromagnetism: Principles and Applications of Bioelectric and Biomagnetic Fields*. London, U.K.: Oxford Univ. Press, 1995.

[35] J. Schmidt, R. Laarousi, W. Stolzmann, and K. Karrer-Gauß, "Eye blink detection for different driver states in conditionally automated driving and manual driving using EOG and a driver camera," *Behav. Res. Methods*, vol. 50, no. 3, pp. 1088–1101, 2018.

[36] X. Zhu, W.-L. Zheng, B.-L. Lu, X. Chen, S. Chen, and C. Wang, "EOG-based drowsiness detection using convolutional neural networks," in *Proc. IJCNN*, 2014, pp. 128–134.

[37] A. Bulling, J. A. Ward, H. Gellersen, and G. Troster, "Eye movement analysis for activity recognition using electrooculography," *IEEE Trans. Pattern Anal. Mach. Intell.*, vol. 33, no. 4, pp. 741–753, Apr. 2011.

[38] Y.-F. Zhang, X.-Y. Gao, J.-Y. Zhu, W.-L. Zheng, and B.-L. Lu, "A novel approach to driving fatigue detection using forehead EOG," in *Proc. 7th Int. IEEE/EMBS Conf. Neural Eng. (NER)*, Apr. 2015, pp. 707–710.

[39] W. L. Zheng and B.-L. Lu, "A multimodal approach to estimating vigilance using EEG and forehead EOG," *J. Neural Eng.*, vol. 14, no. 2, p. 026017, Feb. 2017.

[40] C. Craye, A. Rashwan, M. S. Kamel, and F. Karray, "A multi-modal driver fatigue and distraction assessment system," *Int. J. Intell. Transp. Syst. Res.*, vol. 14, no. 3, pp. 173–194, 2016.

[41] H.-T. Wang, Y.-Q. Li, and T.-Y. Yu, "Coordinated control of an intelligen-twheelchair based on a brain–computer interface and speech recognition," *J. Zhejiang Univ. Sci. C*, vol. 15, no. 10, pp. 832–838, 2014.

[42] H. Wang, Y. Li, J. Long, T. Yu, and Z. Gu, "An asynchronous wheelchair control by hybrid EEG–EOG brain–computer interface," *Cognit. Neurodyn.*, vol. 8, no. 5, pp. 399–409, 2014.

[43] S. K. D'mello and J. Kory, "A review and meta-analysis of multimodal affect detection systems," *ACM Comput. Surv.*, vol. 47, no. 3, p. 43, 2015.

[44] U. Herwig, P. Satrapi, and C. Schönfeldt-Lecuona, "Using the international 10-20 EEG system for positioning of transcranial magnetic stimulation," *Brain Topogr.*, vol. 16, no. 2, pp. 95–99, 2003.

[45] A. Delorme and S. Makeig, "EEGLAB: An open source toolbox for analysis of single-trial EEG dynamics including independent component analysis," *J. Neurosci. Methods*, vol. 134, no. 1, pp. 9–21, Mar. 2004.

[46] K. A. Ludwig, R. M. Miriani, N. B. Langhals, M. D. Joseph, D. J. Anderson, and D. R. Kipke, "Using a common average reference to improve cortical neuron recordings from microelectrode arrays," *J. Neurophysiol.*, vol. 101, no. 3, pp. 1679–1689, 2009.

[47] G. G. Amiri and A. Asadi, "Comparison of different methods of wavelet and wavelet packet transform in processing ground motion records," *Int. J. Civil Eng.*, vol. 7, no. 4, pp. 248–257, 2009.

[48] O. Rosso, M. Martin, and A. Plastino, "Brain electrical activity analysis using wavelet-based informational tools," *Physica A, Stat. Mech. Appl.*, vol. 313, no. 3, pp. 587–608, 2002.

[49] R. R. Coifman, Y. Meyer, S. Quake, and M. V. Wickerhauser, "Signal processing and compression with wavelet packets," in *Wavelets and Their Applications*. Springer, 1994, pp. 363–379.

[50] C. S. Burrus, R. A. Gopinath, and H. Guo, *Introduction to Wavelets and Wavelet Transforms: A Primer*. 1997.

[51] A. R. Hassan, S. Siuly, and Y. Zhang, "Epileptic seizure detection in EEG signals using tunable-Q factor wavelet transform and bootstrap aggregating," *Comput. Methods Programs Biomed.*, vol. 137, pp. 247–259, Dec. 2016.

[52] A. R. Hassan and M. I. H. Bhuiyan, "A decision support system for automatic sleep staging from EEG signals using tunable Q-factor wavelet transform and spectral features," *J. Neurosci. Methods*, vol. 271, pp. 107–118, Sep. 2016.

[53] S. M. Pincus, "Approximate entropy as a measure of system complexity," *Proc. Nat. Acad. Sci. USA*, vol. 88, pp. 2297–2301, Mar. 1991.

[54] J. S. Richman and J. R. Moorman, "Physiological time-series analysis using approximate entropy and sample entropy," *Amer. J. Physiol.-Heart Circulatory Physiol.*, vol. 278, no. 6, pp. 2039–2049, 2000.

[55] R. Zhang *et al.*, "Predicting inter-session performance of SMR-based brain–computer interface using the spectral entropy of resting-state EEG," *Brain Topogr.*, vol. 28, no. 5, pp. 680–690, 2015.

[56] M. Akin and M. K. Kiymik, "Application of periodogram and ar spectral analysis to EEG signals," *J. Med. Syst.*, vol. 24, no. 4, pp. 247–256, 2000.

[57] X. Li, X. Shang, A. Morales-Esteban, and Z. Wang, "Identifying P phase arrival of weak events: The Akaike information criterion picking application based on the empirical mode decomposition," *Comput. Geosci.*, vol. 100, pp. 57–66, Mar. 2017.

[58] M. E. Tipping *et al.*, "Fast marginal likelihood maximisation for sparse Bayesian models," in *Proc. AISTATS*, 2003.

[59] L. Qi and J. Sun, "A nonsmooth version of Newton's method," *Math. Program.*, vol. 58, nos. 1–3, pp. 353–367, 1993.

[60] N. I. Abbasi, I. P. Bodala, A. Bezerianos, Y. Sun, H. Al-Nashash, and N. V. Thakor, "Role of multisensory stimuli in vigilance enhancement—A single trial event related potential study," in *Proc. 39th Annu. Int. Conf. IEEE Eng. Med. Biol. Soc. (EMBC)*, 2017, pp. 2446–2449.

[61] I. P. Bodala, N. I. Abbasi, Y. Sun, A. Bezerianos, H. Al-Nashash, and N. V. Thakor, "Measuring vigilance decrement using computer vision assisted eye tracking in dynamic naturalistic environments," in *Proc. 39th Annu. Int. Conf. IEEE Eng. Med. Biol. Soc. (EMBC)*, Jul. 2017, pp. 2478–2481.

[62] S. G. Hart and L. E. Staveland, "Development of NASA-TLX (Task Load Index): Results of empirical and theoretical research," *Adv. Psychol.*, vol. 52, pp. 139–183, Apr. 1988.
[63] R. Kohavi *et al.*, "A study of cross-validation and bootstrap for accuracy estimation and model selection," in *Proc. Int. Joint Conf. AI*, Aug. 1995, vol. 14, no. 2, pp. 1137–1145.
[64] P. Baldi and A. D. Long, "A bayesian framework for the analysis of microarray expression data: Regularized t-test and statistical inferences of gene changes," *Bioinformatics*, vol. 17, no. 6, pp. 509–519, 2001.
[65] J. A. Hanley, "Receiver operating characteristic (ROC) methodology: The state of the art," *Crit. Rev. Diagnostic Imag.*, vol. 29, no. 3, pp. 307–335, 1989.
[66] S. K. L. Lal and A. Craig, "A critical review of the psychophysiology of driver fatigue," *Biol. Psychol.*, vol. 55, no. 3, pp. 173–194, Feb. 2001.
[67] H. M. Lee, C. M. Chen, J. M. Chen, and Y. L. Jou, "An efficient fuzzy classifier with feature selection based on fuzzy entropy," *IEEE Trans. Syst., Man, Cybern. C, Appl. Rev.*, vol. 31, no. 3, pp. 426–432, Jun. 2001.
[68] S. Nalband, A. Sundar, A. A. Prince, and A. Agarwal, "Feature selection and classification methodology for the detection of knee-joint disorders," *Comput. Methods Programs Biomed.*, vol. 127, pp. 94–104, Apr. 2016.
[69] W. Tao, J. Hai, and L. Liu, "Object segmentation using ant colony optimization algorithm and fuzzy entropy," *Pattern Recognit. Lett.*, vol. 28, no. 7, pp. 788–796, 2007.
[70] A. G. Correa, L. Orosco, and E. Laciar, "Automatic detection of drowsiness in EEG records based on multimodal analysis," *Med. Eng. Phys.*, vol. 36, no. 2, pp. 244–249, 2014.
[71] L.-W. Ko *et al.*, "Single channel wireless EEG device for real-time fatigue level detection," in *Proc. Int. Joint Conf. Neural Netw. (IJCNN)*, Jul. 2015, pp. 1–5.
[72] Y. Xiong, J. Gao, Y. Yang, X. Yu, and W. Huang, "Classifying driving fatigue based on combined entropy measure using EEG signals," *Int. J. Control Autom.*, vol. 9, no. 3, pp. 329–338, 2016.
[73] R. Chai *et al.*, "Improving EEG-based driver fatigue classification using sparse-deep belief networks," *Front. Neurosci.*, vol. 11, p. 103, Mar. 2017.
[74] T. Nguyen, S. Ahn, H. Jang, S. C. Jun, and J. G. Kim, "Utilization of a combined eeg/nirs system to predict driver drowsiness," *Sci. Rep.*, vol. 7, p. 43933, Mar. 2017.
[75] J. Hu and J. Min, "Automated detection of driver fatigue based on EEG signals using gradient boosting decision tree model," *Cognit. Neurodyn.*, vol. 12, no. 4, pp. 431–440, 2018.

HONGTAO WANG (M'17) received the B.S. degree in automatic control from the Guangxi University of Technology, China, in 2004, the M.S. degree in control theory and control engineering from the Wuhan University of Technology, China, in 2007, and the Ph.D. degree in pattern recognition and intelligent systems from the South China University of Technology, China, in 2015.

Since 2013, he has been with the Faculty of Intelligent Manufacturing, Wuyi University, as an Associate Professor. He is also the Director of the Jiangmen Brain-like Computation and Hybrid Intelligence R&D Center. Since 2017, he has also been with the Singapore Institute for Neurotechnology (SINAPSE), Centre for Life Sciences, National University of Singapore, as a Visiting Research Fellow. His research interests include brain-like computation, pattern recognition, and hybrid intelligence.

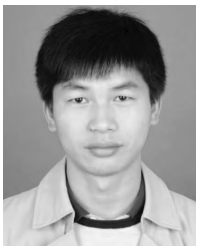

CONG WU was born in Hubei, China, in 1992. He received the bachelor's degree from the School of Electronic Information Science and Technology, Hubei University of Arts and Sciences, China, in 2016. He is currently pursuing the master's degree with the Faculty of Intelligent Manufacturing, Wuyi University.

His research interests include pattern recognition and brain machine interface.

TING LI received the B.S. degree in automatic control from the Taiyuan Machinery College, China, in 1984, the M.S. degree in control theory and control engineering from Northwestern Polytechnical University, Xi'an, China, in 1994, and the Ph.D. degree in mechanical and electrical engineering from the Beijing Institute of Technology, Beijing, China, in 2002.

Since 2002, he has been with the Faculty of Intelligent Manufacturing, Wuyi University, as a Professor. His research interests include pattern recognition and signal processing.

YUEBANG HE was born in Jiangxi, China, in 1983. He received the B.S. degree from the School of Automation Science and Engineering, South China University of Technology, Guangzhou, China, in 2005, and the Ph.D. degree in control theory and applications from the South China University of Technology, Guangzhou, China, in 2013.

Since 2013, he has been with the Faculty of Intelligent Manufacturing, Wuyi University, as a Lecturer. His research interests include robust control, nonlinear control, and UAV automatic control.

PENG CHEN was born in Guangdong, China, in 1979. He received the B.S. degree from the School of Electronics and Information, South China University of Technology, Guangzhou, China, in 2001, and the Ph.D. degree in electronic circuit and system from the South China University of Technology, Guangzhou, China, in 2006.

Since 2006, he has been with the Faculty of Intelligent Manufacturing, Wuyi University, as a Lecturer. His research interests include measurement, signal processing, and automatic control.

ANASTASIOS BEZERIANOS received the degree in physics from Patras University and Telecommunications at Athens University, and the Ph.D. degree in bioengineering from the University of Patras. He has been the Professor of medical physics with the Medical School, Patras University, Patras, Greece, since 2004. He is currently the Head of the Cognitive Engineering (COGEN) Laboratory, Singapore Institute for Neurotechnology (SINAPSE), also a Research Professor with the Electrical and Computer Engineering (ECE) Department, National University of Singapore (NUS), a Professor with the NUS Graduate School for Integrative Sciences and Engineering, and a Visiting Professor with the Computer Science Department, NSWU, Canberra, Australia. He is also the Founder and the Chairman of the Biannual International Summer School on Emerging Technologies in Biomedicine. He has research collaborations with research institutes and universities in Japan, China, and Europe. His work is summarized in 127 journals, one book, 206 conference proceedings publication, and holds two patents. His research interests include artificial intelligence and robotics to biomedical signal processing, brain imaging, mathematical biology, and systems medicine and bioinformatics. He is a Fellow of European Alliance for Medical and Biological Engineering and Science (EAMBES). He is an Associate Editor of the IEEE TNSRE, the *Annals of Biomedical Engineering*, and *PLOS ONE Neuroscience* journals, and a Reviewer for several international scientific journals. He is a Registered Expert of the Horizon 2020 Program of the European Union and of research grant proposals in Greece, Italy, Cyprus, and Canada.